



## Enhanced removal of trace Cr(VI) ions from aqueous solution by titanium oxide–Ag composite adsorbents

Si Si Liu, Yong Zhou Chen, Li De Zhang\*, Guo Min Hua, Wei Xu, Nian Li, Ye Zhang

Key Laboratory of Materials Physics, Anhui Key Laboratory of Nanomaterials and Nanostructure, Institute of Solid State Physics, Hefei Institutes of Physical Science, Chinese Academy of Sciences, Hefei 230031, PR China

### ARTICLE INFO

#### Article history:

Received 20 December 2010  
Received in revised form 29 March 2011  
Accepted 29 March 2011  
Available online 8 April 2011

#### Keywords:

Titanium oxide–Ag composite  
Adsorbent  
Trace  
Cr(VI) removal

### ABSTRACT

Titanium oxide–Ag composite (TOAC) adsorbents were prepared by a facile solution route with Ag nanoparticles being homogeneously dispersed on layered titanium oxide materials. The as-synthesized TOAC exhibited a remarkable capability for trace Cr(VI) removal from an aqueous solution, where the concentration of Cr(VI) could be decreased to a level below 0.05 mg/L within 1 h. We have systematically investigated the factors that influenced the adsorption of Cr(VI), for example, the pH value of the solution, and the contact time of TOAC with Cr(VI). We found that the adsorption of Cr(VI) was strongly pH-dependent. The adsorption behavior of Cr(VI) onto TOAC fitted well the Langmuir isotherm and a maximum adsorption capacity of Cr(VI) as 25.7 mg/g was achieved. The adsorption process followed the pseudo-second-order kinetic model, which implied that the adsorption was composed of two steps: the adsorption of Cr(VI) ions onto TOAC followed by the reduction of Cr(VI) to Cr(III) by Ag nanoparticles. Our results revealed that TOAC with high capacity of Cr(VI) removal had promising potential for wastewater treatment.

© 2011 Elsevier B.V. All rights reserved.

### 1. Introduction

The treatment of industrial wastewater has stimulated worldwide research interest. Industrial wastewater normally contains toxic heavy metals, such as cadmium, mercury, lead, and chromium [1,2], among which chromium poses the most severe environmental concerns. Chromium usually exists in the form of Cr(VI) and Cr(III), where Cr(VI) is more toxic than Cr(III) because of its solubility within almost the whole pH range and its larger mobility than that of Cr(III) [2].

Several treatment techniques have been developed to remove Cr(VI) from wastewater, such as chemical precipitation [3], ion exchange [4,5], membrane technologies [6], and adsorption. Among these techniques, adsorption has become by far the most versatile and widely used one because of its high efficiency and environment-benign characteristics. Sorbents such as acid-treated activated carbons [7–9] and biosorbents [10–14] have been reported to effectively remove Cr(VI) from an aqueous medium. The mechanisms for Cr(VI) removal from the literature can be divided into two categories: (1) the surface reduction of Cr(VI) to Cr(III) followed by the adsorption of Cr(III); (2) the direct adsorption of Cr(VI) anions [15,16]. Although remarkable progress has been achieved,

most of these materials still suffer from several constraints. Activated carbons, one of the most commonly used adsorbents, cannot be regenerated, which leads to high reaction cost and a disposal problem of the solid waste. Biosorbent is economically appealing because of its low cost; however, its removal capacity is limited and the problem of secondary pollution is involved. Therefore, novel highly effective adsorbent materials with enlarged surface charge density and renewable reducing agent should be explored to deal with Cr(VI) at trace level.

Ag nanoparticles have been extensively studied because of its outstanding redox activity and renewability [17,18]. Likewise, titanium oxide and titanium oxide-based materials with large specific surface areas [19,20] have become more and more attractive owing to the high catalysis activity [21] and the strong ion exchange capability [22,23]. These characteristics enable the above materials with the potential as an effective adsorbent. However, so far, there have been only a few reports on titanium oxide or titanium oxide-based adsorbents. Nie and Teh [20] showed that titanate nanotubes ruptured in the adsorption process, resulting in two distinct adsorption stages with adsorption mechanisms of ion exchange and electrostatic attraction respectively, and the maximum adsorption capacity of Pb(II) was 3.752 mmol/g. Liu et al. [24] showed that the titanate nanotubes might be a good adsorbent for the removal of Cu(II) ions from an aqueous solution with the adsorption capacity reaching 120 mg/g.

\* Corresponding author. Tel.: +86 551 5591420; fax: +86 551 5591434.  
E-mail address: [ldzhang@issp.ac.cn](mailto:ldzhang@issp.ac.cn) (L. De Zhang).

Here we show that TOAC could be synthesized via a facile solution route, and the composite adsorbents can effectively adsorb trace Cr(VI) and enable the transformation of the toxic Cr(VI) to the harmless Cr(III) by the action of redox-active Ag nanoparticles. TOAC before and after adsorption were characterized by X-ray diffraction (XRD) and X-ray photoelectron spectroscopy (XPS). Adsorption of Cr(VI) onto TOAC was tested as a function of solution pH value, and contact time. The kinetics of Cr(VI) uptake by TOAC was examined with respect to pseudo-second-order kinetic model. The Langmuir adsorption equation was used to fit the experimental data. Additionally, the regeneration of TOAC was also investigated in detail.

## 2. Experimental

### 2.1. Materials

Metatitanic acid ( $\text{TiO}(\text{OH})_2$ ,  $\text{TiO}_2$  content 80%) was used to fabricate the layered titanium oxide (LTO) without any further purification. Aqueous solutions containing Cr(VI) were prepared by dissolution of  $\text{K}_2\text{Cr}_2\text{O}_7$  in deionized (DI) water. NaOH, HCl,  $\text{AgNO}_3$ , ascorbic acid,  $\text{NH}_3\text{OH}$ , Polyvinylpyrrolidone (PVP), and 1,5-diphenylcarbazine (DPC) were of analytical grade, and purchased from Alfa Aesar. The commercial activated carbon (Flitrasorb100, Calgon) was used in this work for comparison. Deionized water (resistivity  $\geq 18.0 \text{ M}\Omega \text{ cm}$ ) was used for all the experiments.

### 2.2. Preparation of layered titanium oxide

LTO was prepared by a hydrothermal method. In a typical synthetic process, 3 g of metatitanic acid was mixed with 40 mL NaOH (10 M) in a 50 mL Teflon-lined autoclave container by stirring for 1 h at the ambient temperature to uniformly disperse the reagents in the solution, followed by heating in an oven at  $80^\circ\text{C}$  for 24 h. The product of the reaction was filtrated and cleaned several times with 0.1 M HCl and DI water until the filtrate was neutral. The obtained LTO was dried at  $80^\circ\text{C}$  for 24 h.

### 2.3. Preparation of titanium oxide–Ag composite (TOAC)

A mixture of 0.75 g PVP and 2 g LTO was suspended in 100 mL DI water, and 10 mL  $[\text{Ag}(\text{NH}_3)_2]\text{NO}_3$  solution (10 g/L) was added subsequently. After stirring at the ambient temperature for 24 h, the mixture was washed with DI water several times and transferred into a 250 mL conical beaker. The purpose of adding PVP was to control the growth and agglomeration of Ag nanoparticles. 15 mL ascorbic acid (10 g/L) was slowly added into the above suspension to reduce Ag(I), followed by stirring for 5 h. The obtained product was washed thoroughly with DI water and dried in the oven under vacuum at  $80^\circ\text{C}$  for 24 h.

### 2.4. Characterization

The specific surface areas of LTO and TOAC were determined by nitrogen adsorption by using a five-point BET isotherm (ASAP 2010 system, Micromeritics Instrument Corp.). The morphologies of samples were characterized by scanning electron microscopy (SEM, Sirion 200) and transmission electron microscopy (TEM). XRD patterns were recorded on a diffractometer with the  $\text{Cu K}\alpha$  radiation (X'Pert Pro MPD, Philips). The Zeta potential was measured using a Zeta-Meter (Zetasizer 3000HSA, Malvern). XPS of TOAC before and after adsorption were obtained by an ESCALab220i-XL electron spectrometer from VG Scientific using 300 W Al  $\text{K}\alpha$  radiation, where the binding energies were referenced to the C1 s line at 284.8 eV from adventitious carbon. The concentration of Cr(VI) was determined colorimetrically by measuring the intense red–violet

complex formed by reaction of chromium(VI) with DPC in an acidic medium. A UV–vis Spectrometer (Cary 50, Varian) was used to measure the absorption of chromophore complex at its absorbance maximum of 540 nm [25].

### 2.5. Adsorption experiments

Batch adsorption experiments were conducted in 100 mL conical beakers containing 60 mL of various concentrations of Cr(VI) solutions at room temperature ( $25^\circ\text{C}$ ). The conical beakers were

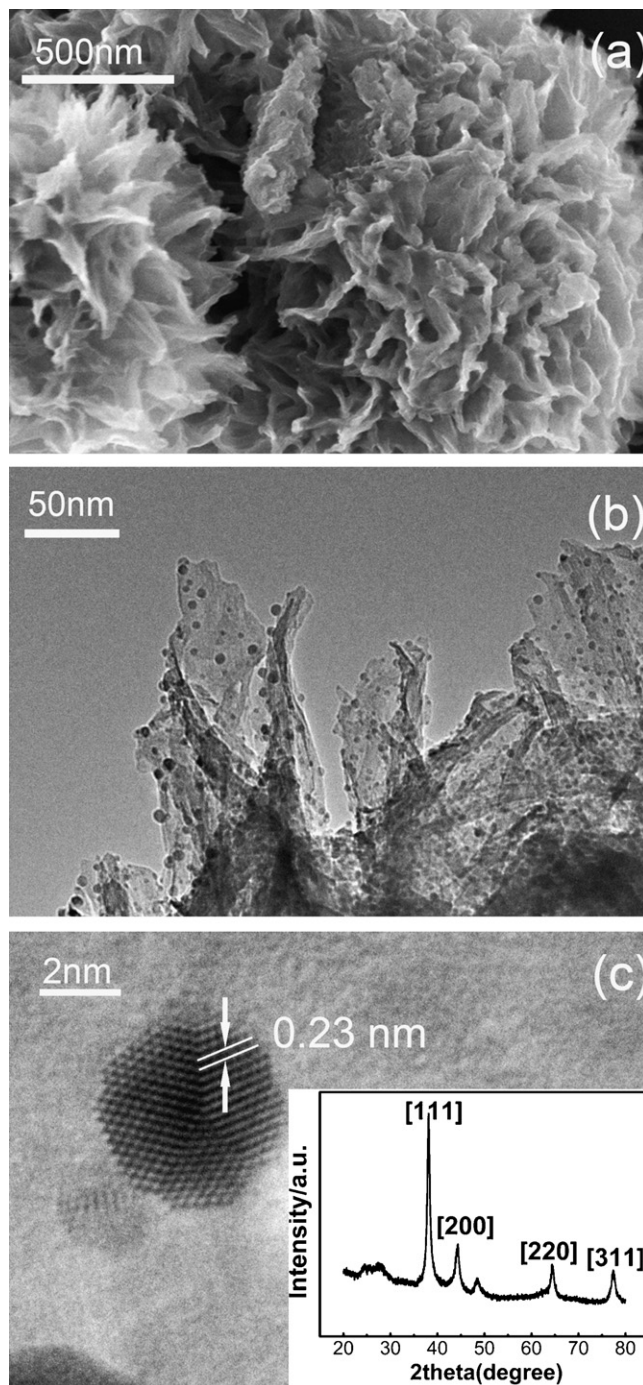


**Fig. 1.** (a) The SEM image of the titanium oxide–Ag composite; (b) the TEM image of titanium oxide–Ag composite; (c) the TEM image of Ag nanoparticles on the surface of layered titanium oxide (inset is an XRD pattern of Ag nanoparticles on the surface of titanium oxide).

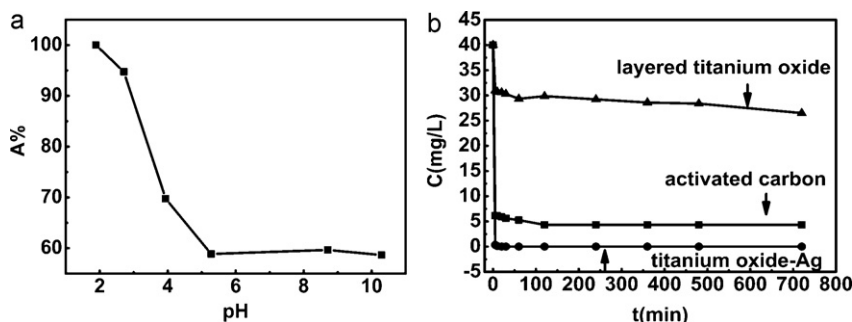


Fig. 2. Effect of (a) the pH value on the removal efficiency (A%) of Cr(VI) by titanium oxide-Ag composite; (b) the concentration (C) of Cr(VI) with the contact time for layered titanium oxide, activated carbon, and titanium oxide-Ag composite, respectively.

agitated at 100 rpm in a thermostatic shaking incubator (TS-100B, Tensuc Shanghai) to reach the equilibrium. After adsorption, all the solution samples were centrifuged at 8500 rpm for 5 min, and the up-clear solution was taken for the Cr(VI) concentration measurements.

The effect of the pH value on the adsorption of Cr(VI) by TOAC was investigated under following conditions. The initial pH values of Cr(VI) solutions (40 mg/L) were adjusted to 2.0–10.0 by adding 0.1 M HCl or 0.1 M NaOH solution. The solutions were then mixed with 0.2 g TOAC in 100 mL conical beakers and agitated for 12 h. Only the optimum pH would be used in the further study.

The effect of contact time on adsorption capability of LTO, TOAC or activated carbon was studied at an initial Cr(VI) concentration of 40 mg/L with the adsorbent dosage of 0.2 g at pH 2. During the experiments, the aliquots of water samples were withdrawn in the range of 5–720 min and the Cr(VI) concentration in each of the water samples was determined. The study of the adsorption isotherm was conducted by adding 0.1 g TOAC into various initial concentrations of Cr(VI) ions in the range of 30–80 mg/L at pH 2 and agitating for 12 h.

### 2.6. Regeneration of adsorbents

All the residual adsorbents were collected and soaked into  $\text{NH}_3 \cdot \text{H}_2\text{O}$  for 24 h. After rinsing with DI water for several times, the residual adsorbents were transferred into 100 mL DI water. Subsequently, ascorbic acid solution with a concentration of 10 g/L was slowly added into the suspension to regenerate TOAC. The obtained black product was washed thoroughly with DI water and dried in the oven under vacuum at 80 °C for 24 h. The method of testing the capability of regenerated samples was the same as the adsorption experiments above.

## 3. Results

### 3.1. Characterization of adsorbents

Fig. 1a shows the SEM image of LTO prior to being loaded with Ag nanoparticles. It can be observed that LTO sheets are assembled together to form a flowerlike shape (The  $\text{N}_2$ -BET surface area was measured as 404  $\text{m}^2/\text{g}$ ). This result indicates that LTO has a large specific surface area, which can provide a large number of active sites for reaction. Fig. 1b shows the TEM image of TOAC. It reveals that a large number of Ag nanoparticles are homogeneously dispersed on the surface of LTO (The  $\text{N}_2$ -BET surface area was measured as 209  $\text{m}^2/\text{g}$ ). From the high-magnification TEM image in Fig. 1c, the average diameter of Ag nanoparticles is about 5 nm. The crystal lattice fringe of Ag nanoparticles with d spacing of 0.23 nm corresponds to (1 1 1) planes of Ag. Inset in Fig. 1c shows the XRD pattern of TOAC. The diffraction peaks at  $2\theta = 38.1^\circ$ ,  $44.3^\circ$ ,  $64.5^\circ$ , and  $77.3^\circ$  can be indexed to (1 1 1), (2 0 0), (2 2 0), and (3 1 1) planes of

face-centered cubic Ag (JCPDS No. 04-0783), respectively. The two broad and weak diffraction peaks in the XRD pattern indicate that LTO is amorphous.

### 3.2. Adsorption behavior of Cr(VI) onto the adsorbents

#### 3.2.1. Effect of the pH value

Fig. 2a shows the Cr(VI) removal efficiency of TOAC at different pH values, ranging from 2.0 to 10.0. The removal efficiency A (%) is defined as follows:

$$A(\%) = \left(1 - \frac{c_e}{c_0}\right) \times 100 \quad (1)$$

where  $c_0$  and  $c_e$  are the initial and equilibrium concentrations of Cr(VI), respectively. The removal efficiency of Cr(VI) decreases swiftly with pH from 2 to 5, and then stays as a constant above pH 5, which implies that the adsorption of Cr(VI) is strongly dependent on the pH value of the solution. The point of zero charge (PZC) of TOAC is determined to be about 5.3, which means that TOAC has an enlarged surface charge density with decreasing pH from 5 to 2, resulting in a strong electrostatic attraction between the adsorbents and the anionic adsorbates. TOAC with positive charges shows greater tendency to adsorb anions. Hence, pH 2.0 is fixed as the optimum value for further adsorption studies.

#### 3.2.2. Effect of the contact time

The change of the concentration of Cr(VI) with the contact time is graphically presented in Fig. 2b. It is observed that the concentration of Cr(VI) initially decreases with the contact time, and then reaches the equilibrium state in 12 h. It is noticed that the concentration of Cr(VI) is rapidly decreased to below 0.05 mg/L by TOAC within 1 h. As a comparison, it is only decreased to 30 mg/L and 5 mg/L, respectively, by LTO and activated carbon with the same amount. These significant differences of removal capability among TOAC, LTO, and active carbon can be explained by considering the fact that removal capability is affected by the ratio of the number of adsorption sites to the number of metal species. Due to surface modification, the number of adsorption sites of TOAC and its positive charges on the surface has increased dramatically. Consequently, adsorption of Cr(VI) ions onto TOAC proceeds rapidly as more Cr(VI) ions are adsorbed through columbic force at acidic condition. It is evident that TOAC shows more remarkable removal capability of Cr(VI) ions than active carbon which only reduces the concentration of Cr(VI) to above 5 mg/L.

#### 3.2.3. Langmuir adsorption isotherm

In order to understand in-depth and clarify the adsorption processes, the adsorption mechanism of Cr(VI) ions onto TOAC is investigated. The experimental results can be well fitted by the Langmuir isotherm equation (Fig. 3a), which indicates that the adsorption of Cr(VI) ions belongs to monolayer adsorption in this

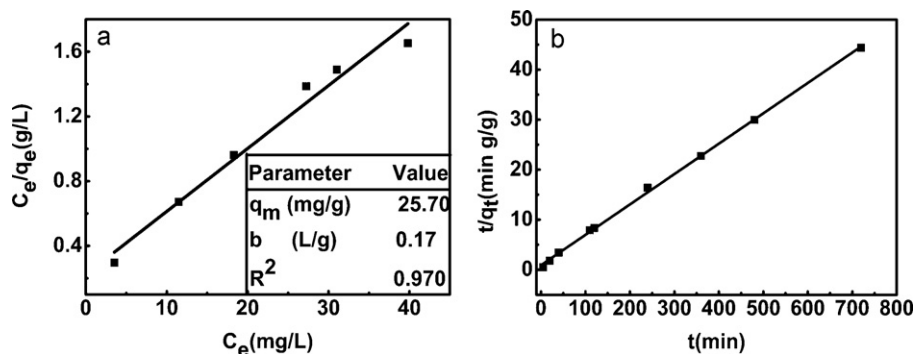


Fig. 3. (a) Langmuir adsorption isotherms of Cr(VI) for the Cr(VI) adsorbent of titanium oxide–Ag composite; (b) the pseudo-second-order kinetic model for adsorption of Cr(VI) by titanium oxide–Ag composite.

study. As for the Langmuir isotherm equation, it can be described as follows [26]:

$$q_e = V \frac{C_0 - C_e}{m} \quad (2)$$

$$\frac{C_e}{q_e} = \frac{1}{q_m b} + \frac{C_e}{q_m} \quad (3)$$

where  $b$  (L/mg) is the Langmuir constant related to the rate of adsorption and  $q_m$  is the theoretical monolayer saturation capacity (mg/g). From the fitted Langmuir isotherm equation,  $q_m$  is obtained as 25.7 mg/g.

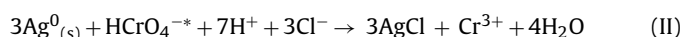
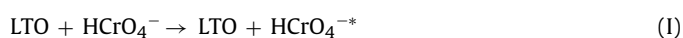
### 3.2.4. Adsorption kinetics analysis

Kinetic model is helpful to understand the kinetic processes of metal ions adsorption and evaluate the performance of the adsorbents for metal removal. The pseudo-second-order kinetic model is successfully applied to evaluate the Cr(VI) adsorption kinetics on TOAC. It can be expressed as [27]:

$$\frac{t}{q_t} = \frac{1}{k_2 q_e^2} + \frac{t}{q_e} \quad h = k_2 q_e^2 \quad (4)$$

where  $q_t$  is the amount of adsorbate adsorbed per unit mass of adsorbent during the period of time  $t$  (mg/g),  $k_2$  is the equilibrium rate constant for the pseudo-second-order (g/mg min), and  $h$  is the initial adsorption rate (mg/g h). These constants can be determined by fitting the curve of  $t/q_t$  against  $t$ . Fig. 3b shows the linear relation between  $t/q_t$  and  $t$ , where the fitted values of  $k_2$  and  $h$  are 0.051 g/mg h and 19.845 mg/g h, respectively. The  $R^2$  value for the pseudo-second-order kinetic model is 0.999. Thus, the system under study is more appropriately described by the pseudo-second-order model, which means that the removal of Cr(VI) proceeds in two steps: firstly, the electrostatic force attracts Cr(VI) ions towards LTO; secondly, Cr(VI) ions are reduced to Cr(III)

ions by Ag nanoparticles. The chemical reaction equations are described as follows:



where  $\text{HCrO}_4^{*-}$  represents the adsorption state of  $\text{HCrO}_4^-$  on LTO.  $\text{Cl}^-$  comes from HCl solution which is used for pH modulation.

### 3.2.5. XPS characterization

To verify the chemical reactions conducted on the surface of TOAC, the samples are characterized by high-resolution XPS. According to previous literatures [28], the bonding energy value of Ag 3d<sub>5/2</sub> signal reported for Ag<sup>0</sup> nanoparticles is around 367.9 eV. The XPS spectrum in the Ag 3d region of TOAC before adsorption is presented in Fig. 4a, where the value of Ag 3d<sub>5/2</sub> is 367.6 eV. The peak shifts towards the lower binding energy is attributed to the strong Ag:O and Ag:N coordination because of the donation of lone pair electrons to sp orbitals of silver from C=O and C–N in PVP [29,30]. From Fig. 4b, the Cl 2p<sub>3/2</sub> peak is observed at 197.3 eV. This result reveals the existence of AgCl on the surface of TOAC after adsorption. The XRD pattern of TOAC after adsorption is also shown in the inset in Fig. 4b. Apart from the peaks related to metallic Ag, the remaining peaks correspond to the diffraction peaks of AgCl (JCPDS No. 01-1013), which confirms the formation of AgCl after adsorption of Cr(VI) ions. These findings imply that Ag nanoparticles serving as the electron reservoir can effectively reduce Cr(VI) to Cr(III) in the adsorption processes. Simultaneously, Ag nanoparticles are oxidized to Ag<sup>+</sup> ions that interacted with Cl<sup>−</sup> ions on the surface to form AgCl (see chemical reaction (II)).

The high-resolution Cr 2p<sub>3/2</sub> and Cr 2p<sub>1/2</sub> XPS spectrum for TOAC after adsorption of Cr(VI) ions (Fig. 4c) shows that Cr 2p<sub>3/2</sub> and Cr 2p<sub>1/2</sub> peaks appear at 577.4 eV and 580.1 eV, respectively. These bonding energies are in good agreement with the results obtained by Carver [31] and Shuttleworth [32]. Quantitative curve fitting was

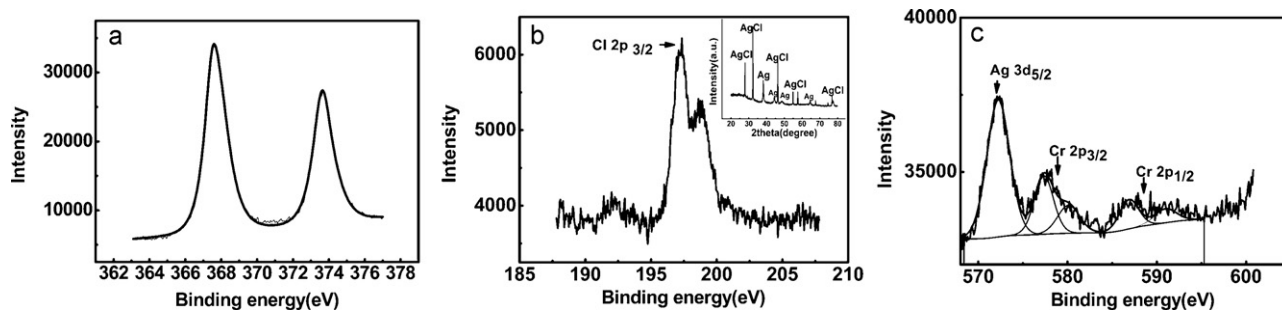


Fig. 4. XPS spectrum of Ag 3d before (a) and Cl 2p; (b) after adsorption of Cr(VI) ions (inset is an XRD pattern of a sample after adsorption); (c) high-resolution Cr 2p XPS spectrum after adsorption of Cr(VI).

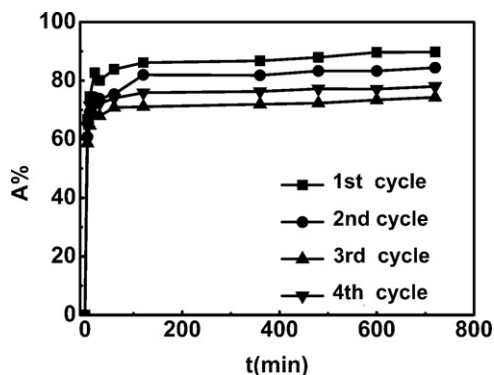


Fig. 5. The removal efficiency of Cr(VI) with the contact time for regenerated titanium oxide–Ag composite.

applied to the XPS spectrum of TOAC with adsorbate of Cr species. The curve fitting result reveals that about 64.5% of the chromium species on the surface is in the Cr(III) state, while about 35.5% is in the Cr(VI) state. The large number of Cr(III) ions observed can be attributed to the high loading density of redox-active Ag<sup>0</sup> nanoparticles on the surface of LTO, which can serve as the electronic reservoir to reduce Cr(VI) ions to Cr(III) ions.

### 3.2.6. Regeneration of adsorbents

Regeneration of adsorbent is significant for the practical wastewater treatments. In order to investigate the cyclic capability of TOAC on the removal of Cr(VI), the residual adsorbents were dipped in NH<sub>3</sub>·H<sub>2</sub>O for 24 h to decompose AgCl into Ag<sup>+</sup> and Cl<sup>-</sup>. The as-generated Ag<sup>+</sup> became Ag(NH<sub>3</sub>)<sub>2</sub><sup>+</sup> and adsorbed on the surface of LTO in the alkaline environment. Ag nanoparticles were regenerated via reduction of Ag(I) by ascorbic acid. Fig. 5 shows the effect of contact time on the performance of the regenerated TOAC. It is found that the removal rate of Cr(VI) is also high within 2 h and the removal efficiencies of Cr(VI) on those four cycles are around 80%, which indicate the feasibility of regeneration of TOAC.

## 4. Discussion

From the results presented in the previous section, we notice that TOAC provides a high positive surface charge density which leads to enhanced removal capability for Cr(VI) ions. Meanwhile, the comparison experiment of TOAC and activated carbon indicates that TOAC adsorbent can be used to deal with heavy metal ions at trace level. In general, the enhanced adsorption of trace pollutants could be originated from two aspects: the stronger interaction between the adsorbents and adsorbates and the sufficient anchoring sites to adsorb the trace pollutants and prevent their desorption. We suggest that electrostatic attraction between TOAC and adsorbates is responsible for Cr(VI) removal at trace level, because the concentration gradient is deficient to drive the adsorbates towards the surface of LTO at trace level. However, interfaces between Ag nanoparticles and LTO could provide a large number of stronger anchoring sites for Cr(VI) adsorption. Such adsorption enhancement arising from the interfaces has been observed in the catalyst systems of alumina, ceria, and zirconia-supported noble metal particles [33,34]. Moreover, Cr(VI) ions anchored at the interfaces between Ag nanoparticles and LTO are easily reduced to Cr(III) ions by active Ag nanoparticles.

## 5. Conclusion

Titanium oxide–Ag composites, comprised of Ag nanoparticles loaded on layered titanium oxide, were prepared by a facile solution route. When TOAC was used as an adsorbent to adsorb

Cr(VI) ions in a solution, the adsorption equilibrium state is rapidly reached within 1 h and the Cr(VI) concentration is decreased to below 0.05 mg/L. Batch adsorption studies show that the adsorption capacity of TOAC for the removal of Cr(VI) is strongly dependent on the initial pH value. The adsorption of Cr(VI) by TOAC is well modeled by the Langmuir isotherm and the maximum adsorption capacity of Cr(VI) is calculated as 25.7 mg/g. The adsorption of Cr(VI) follows the pseudo-second-order kinetic model, which implies that the removal process is a chemical adsorption associated with transformation of Cr(VI) ions to Cr(III) ions. Regeneration studies show the feasibility of regeneration of TOAC. In summary, this work has demonstrated that TOAC as an adsorbent has promising potential for trace level heavy metal removal in the wastewater.

## Acknowledgement

This work was financially supported by the National Natural Science Foundation of China (NSFC) (grant no. 10804112) and the National Basic Research Program of China (no. 2011CB933700).

## References

- [1] L.D. Zhang, M. Fang, Nanomaterials in pollution trace detection and environmental improvement, *Nano Today* 5 (2010) 128–142.
- [2] Y.B. Zeng, H.S. Woo, G.H. Lee, J.B. Park, Adsorption of Cr(VI) on hexadecylpyridinium bromide (HDPB) modified natural zeolites, *Microporous Mesoporous Mater.* 130 (2010) 83–91.
- [3] J.W. Paterson, *Wastewater Treatment Technology*, Ann Arbor Science, Michigan, 1975, pp. 43–58.
- [4] G. Tiravanti, D. Petruzzelli, R. Passino, Pretreatment of tannery wastewaters by an ion exchange process for Cr(III) removal and recovery, *Water Sci. Technol.* 36 (1997) 197–207.
- [5] S. Rengaraj, K.H. Yeon, S.H. Moon, Removal of chromium from water and wastewater by ion exchange resins, *J. Hazard. Mater.* 87 (2001) 273–287.
- [6] C.A. Kozłowski, W. Walkowiak, Removal of chromium(VI) from aqueous solutions by polymer inclusion membranes, *Water Res.* 36 (2002) 4870–4876.
- [7] P.K. Ghosh, Hexavalent chromium [Cr(VI)] removal by acid modified waste activated carbons, *J. Hazard. Mater.* 171 (2009) 116–122.
- [8] S.J. Park, Y.S. Jang, Pore structure and surface properties of chemically modified activated carbons for adsorption mechanism and rate of Cr(VI), *J. Colloid Interface Sci.* 249 (2) (2002) 458–463.
- [9] S. Babel, T.A. Kurniawan, Cr(VI) removal from synthetic wastewater using coconut shell charcoal and commercial activated carbon modified with oxidizing agents and/or chitosan, *Chemosphere* 54 (2004) 951–967.
- [10] N. Daneshvar, D. Salari, S. Aber, Chromium adsorption and Cr(VI) reduction to trivalent chromium in aqueous solutions by soya cake, *J. Hazard. Mater. B* 94 (2002) 49–61.
- [11] U.K. Garg, M.P. Kaur, V.K. Garg, D. Sud, Removal of hexavalent chromium from aqueous solution by agricultural waste biomass, *J. Hazard. Mater.* 140 (2007) 60–68.
- [12] C. Raji, T.S. Anirudhan, Batch Cr(VI) removal by polyacrylamide-grafted sawdust: kinetics and thermodynamics, *Water Res.* 32 (12) (1998) 3772–3780.
- [13] R.S. Bai, T.E. Abraham, Studies on enhancement of Cr(VI) biosorption by chemically modified biomass of *Rhizopus nigricans*, *Water Res.* 36 (5) (2002) 1224–1236.
- [14] R.S. Bai, T.E. Abraham, Studies on chromium(VI) adsorption–desorption using immobilized fungal biomass, *Bioresour. Technol.* 87 (1) (2003) 17–26.
- [15] D. Mohan, C.U. Pittman Jr., Activated carbons and low cost adsorbents for remediation of tri and hexavalent chromium from water, *J. Hazard. Mater. B* 137 (2006) 762–811.
- [16] C. Selomulya, V. Meeyoo, R. Amal, Mechanisms of Cr(VI) removal from water by various types of activated carbons, *J. Chem. Technol. Biotechnol.* 74 (2) (1999) 111–122.
- [17] N. Pradhan, A. Pal, A. Pal, Silver nanoparticle catalyzed reduction of aromatic nitro compounds, *Colloids Surf. A* 196 (2002) 247–257.
- [18] M. Andersson, J.S. Pedersen, A.E.C. Palmqvist, Silver nanoparticle formation in microemulsions acting both as template and reducing agent, *Langmuir* 21 (2005) 11387–11396.
- [19] T. Kasuga, M. Hiramatsu, A. Hoson, T. Sekino, K. Niihara, Formation of titanium oxide nanotube, *Langmuir* 14 (1998) 3160–3163.
- [20] X.T. Nie, Y.L. Teh, Titanate nanotubes as superior adsorbents for removal of lead(II) ions from water, *Mater. Chem. Phys.* 123 (2010) 494–497.
- [21] M. Bizarro, M.A. Tapia-Rodríguez, M.L. Ojeda, J.C. Alonso, A. Ortiz, Photocatalytic activity enhancement of TiO<sub>2</sub> films by micro and nano-structured surface modification, *Appl. Surf. Sci.* 255 (2009) 6274–6278.
- [22] J. Yang, D. Li, X. Wang, X. Yang, L. Lu, Study on the synthesis and ion exchange properties of layered titanate Na<sub>2</sub>Ti<sub>3</sub>O<sub>7</sub> powders with different sizes, *J. Mater. Sci.* 38 (2003) 2907–2911.

- [23] X.M. Sun, Y.D. Li, Synthesis and characterization of ion exchangeable titanate nanotubes, *Chem. Eur. J.* 9 (2003) 2229–2238.
- [24] S.S. Liu, C.K. Lee, H.C. Chen, C.C. Wang, L.C. Juang, Application of titanate nanotubes for Cu(II) ions adsorptive removal from aqueous solution, *J. Chem. Eng.* (2009) 188–193.
- [25] ASTM: Annual Book of ASTM Standards, Standard Test Methods for Chromium in Water, D1687-02R07E01, 11.01.2009.
- [26] F.Y. Wang, H. Wang, J.W. Ma, Adsorption of cadmium(II) ions from aqueous solution by a new low-cost adsorbent—bamboo charcoal, *J. Hazard. Mater.* 177 (2010) 300–306.
- [27] A.R. Kula, H. Koyuncu, Adsorption of Pb(II) ions from aqueous solution by native and activated bentonite: kinetic, equilibrium and thermodynamic study, *J. Hazard. Mater.* 179 (2010) 332–339.
- [28] J.C. Fuggle, E. Kallne, L.M. Watson, D.J. Fabian, Electronic structure of aluminum and aluminum-noble-metal alloys studied by soft-X-ray and X-ray photoelectron spectroscopies, *Phys. Rev. B* 16 (1977) 750–761.
- [29] Y.Z. Wang, Y.X. Li, S.T. Yang, G.L. Zhang, D.M. An, C. Wang, Q.B. Yang, X.S. Chen, X.B. Jing, Y. Wei, A convenient route to polyvinyl pyrrolidone/silver nanocomposite by electrospinning, *Nanotechnology* 17 (2006) 3304–3307.
- [30] M. Jin, X.T. Zhang, S. Nishimoto, Z.Y. Liu, D.A. Tryk, T. Murakami, A. Fujishima, Large-scale fabrication of Ag nanoparticles in PVP nanofibres and net-like silver nanofibre films by electrospinning, *Nanotechnology* 18 (2007) 1–7.
- [31] J.C. Carver, G.K. Schweitzer, Use of X-ray photoelectron spectroscopy to study bonding in Cr, Mn, Fe, and Co compounds, *J. Chem. Phys.* 57 (1972) 973.
- [32] D. Shuttleworth, Preparation of metal-polymer dispersions by plasma techniques: an ESCA investigation, *J. Phys. Chem. Solids* 84 (1980) 1629–1634.
- [33] J. Fan, X.D. Wu, R. Ran, D. Weng, Influence of the oxidative/reductive treatments on the activity of Pt/Ce<sub>0.6</sub>Zr<sub>0.33</sub>O<sub>2</sub> catalyst, *Appl. Surf. Sci.* 245 (2005) 162–171.
- [34] J.L. Ayastuy, M.P. González-Marcos, A. Gil-Rodríguez, J.R. González-Velas, M.A. Gutiérrez-Ortiz, Selective CO oxidation over Ce<sub>x</sub>Zr<sub>1-x</sub>O<sub>2</sub>-supported Pt catalysts, *Catal. Today* 116 (2006) 391–399.